
Supplementary Material for ODE²VAE: Deep generative second order ODEs with Bayesian neural networks

Çağatay Yıldız¹, Markus Heinonen^{1,2}, Harri Lähdesmäki¹

Department of Computer Science

Aalto University, Finland, FI-00076

{cagatay.yildiz, markus.o.heinonen, harri.lahdesmaki}@aalto.fi

1 Ablation studies

1st-order baseline: We tested a new ODE¹VAE variant where the latent space is governed by 1st-order ODE system. ODE¹VAE is similar to the NeuralODE [Chen et al. \(2018\)](#), except for having BNNs, and for NeuralODE placing a variational distribution on initial value $q(\mathbf{x}_0)$, while ODE¹VAE models the posterior over full trajectory $q(\mathbf{x}_{0:T})$.

ODE¹VAE vs ODE²VAE: We performed a new comparison study of ODE¹VAE against ODE²VAE on bouncing balls dataset. The experimental setup is kept the same, except that the number of convolutional filters is reduced so that the impact of differential function choice becomes more apparent. Table 1 shows the resulting MSE over 10 frame ahead predictions. Note that ODE²VAE models the acceleration $\dot{\mathbf{v}}_t = \mathbf{f}(\mathbf{s}_t, \mathbf{v}_t) : \mathbb{R}^{2d} \rightarrow \mathbb{R}^d$ whereas 1st-order systems learn $\dot{\mathbf{z}}_t = \mathbf{f}(\mathbf{z}_t) : \mathbb{R}^d \rightarrow \mathbb{R}^d$. Results show that the 2nd-order dynamics results in far better accuracy, even if the first order dynamics has more flops ($d = 50$). We will include ablation studies in the paper.

NN vs BNN: Table 1 shows comparable performance of BNNs and NNs on bouncing balls. In order to demonstrate the benefit of using a BNN, we repeat the CMU walking experiment with a NN differential function. The MSE achieved by ODE²VAE-NN over three test sequences is 9.96, whereas ODE²VAE-BNN error improves to 9.43.

Table 1: Comparison of neural network (NN) and Bayesian neural network (BNN) ODE’s with different latent dimensionalities on BOUNCING BALL experiment. Adding 2nd order momentum achieves superior performance, while BNN’s have a smaller impact.

Model	Latent dimensions d		Test MSE	
	1st-order state	2nd-order momentum	NN	BNN
ODE ¹ VAE	25	-	45	43
	50	-	36	35
ODE ² VAE	25	25	26	27

2 Extra results

Below, we report the MSEs of mean trajectories, which are obtained with mean model predictions (e.g., for our model, when the mean value from the encoder distribution and variational posterior is used).

Table 2: Average mean MSE on future mocap frames

Model	Test error		Reference
	Dataset 1	Dataset 2	
GPDM	57.52	N/A	Wang et al. (2008)
VGPLVM	128.03	N/A	Damianou et al. (2011)
DTsBN-S	78.39	37.20	Gan et al. (2015)
NPODE	45.74	22.96	Heinonen et al. (2018)
NEURALODE	97.74	21.60	Chen et al. (2018)
ODE ² VAE	32.19	17.20	current work
ODE ² VAE-KL	30.72	6.48	current work

Table 3: Mean prediction errors on test angle of rotating MNIST dataset (\diamond taken from [Casale et al. \(2018\)](#))

MODEL	TEST ERROR
GPPVAE-DIS \diamond	0.0306
GPPVAE-JOINT \diamond	0.0280
ODE ² VAE	0.0204
ODE ² VAE-KL	0.0184

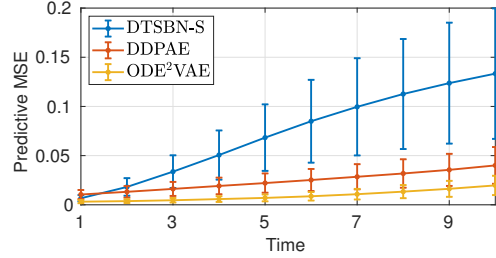


Figure 1: Mean prediction errors on bouncing balls dataset.

3 Experiment details

3.1 CMU mocap

We consider two different datasets. [Here](#) is a link to the first one (with 43 sequences) and [here](#) is a link to the second dataset. We set $\gamma = 1$. We tried out the architecture in Figure 4 with 1/2 hidden layers, 30/50 hidden units, tanh/relu/no activation functions. We found out that 2 hidden layers, 30 units and tanh performs the best. Each experiment is executed on a standard laptop for around 3 hours. The latent dimensionality is fixed to 6 for all models, i.e., $\mathbf{s}_t, \mathbf{v}_t \in \mathbb{R}^3$.

We visualize the position trajectories in Figure 2 for cases in which either encoder/BNN variational posteriors are sampled or the mean values are used. Note that latent field that is considered in our work corresponds to the right-most panel, whereas neural ODEs considers the second one.

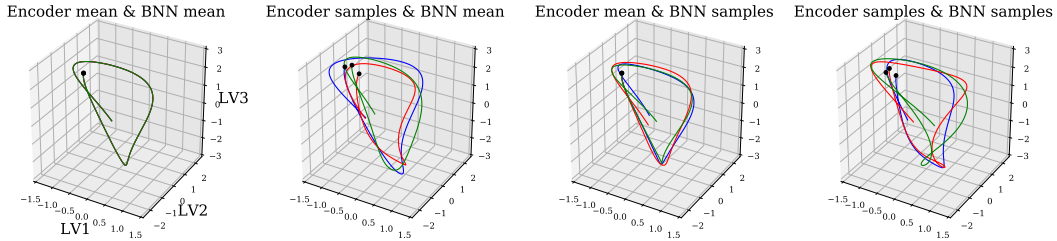


Figure 2: Example latent trajectories from CMU mocap experiment

3.2 Rotating MNIST

[Here](#) is the dataset. We set $\gamma = 1$. We tried out 4/8/12 as the number of layers in the first layers of encoders and 8/12/16 as the last layer of the decoder. The code is executed on NVIDIA Tesla V100 GPUs for around 4 hours. The latent dimensionality is fixed to 16 for all models, i.e., $\mathbf{s}_t, \mathbf{v}_t \in \mathbb{R}^8$.

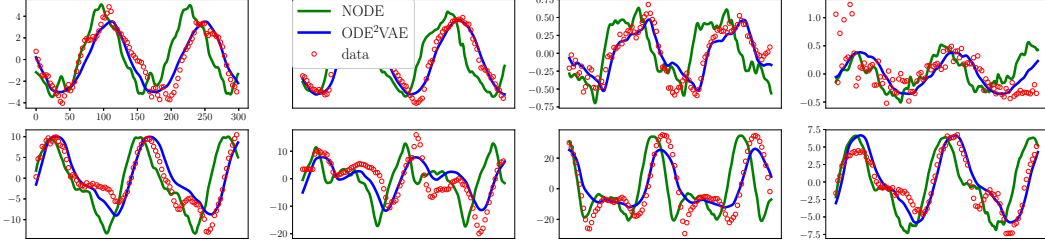


Figure 3: Comparison of our method against neural ODEs on CMU mocap data set. Each panel demonstrates a sensor measurement plotted over time.

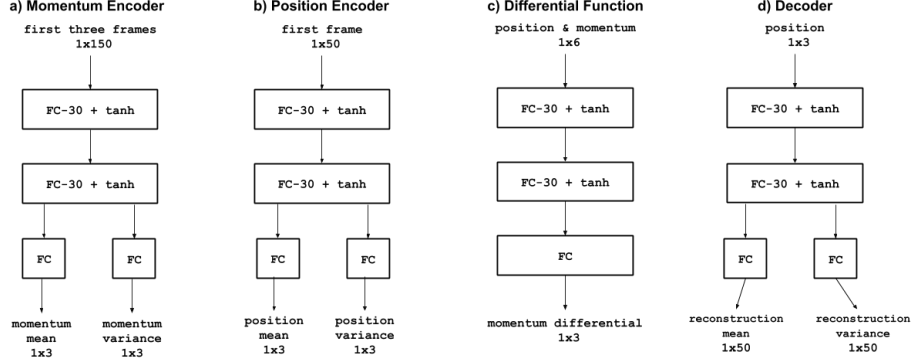


Figure 4: CMU mocap walking data experiment neural architectures

3.3 Bouncing balls

Here is the dataset. We set $\gamma = 0.001$. We tried out 8/16/32 as the number of layers in the first layers of encoders and 16/32 as the last layer of the decoder. We also experimented with relu and tanh activations. The code is executed on NVIDIA Tesla V100 GPUs for around 3 days. The latent dimensionality is fixed to 50 for all models, i.e., $s_t, v_t \in \mathbb{R}^{25}$. Also note that we obtained the same error when $s_t, v_t \in \mathbb{R}^{50}$.

References

- Francesco Paolo Casale, Adrian Dalca, Luca Saglietti, Jennifer Listgarten, and Nicolo Fusi. Gaussian process prior variational autoencoders. In *Advances in Neural Information Processing Systems*, pages 10369–10380, 2018.
- Tian Qi Chen, Yulia Rubanova, Jesse Bettencourt, and David K Duvenaud. Neural ordinary differential equations. In *Advances in Neural Information Processing Systems*, pages 6571–6583, 2018.
- Andreas Damianou, Michalis K Titsias, and Neil D Lawrence. Variational gaussian process dynamical systems. In *Advances in Neural Information Processing Systems*, pages 2510–2518, 2011.
- Zhe Gan, Chunyuan Li, Ricardo Henao, David E Carlson, and Lawrence Carin. Deep temporal sigmoid belief networks for sequence modeling. In *Advances in Neural Information Processing Systems*, pages 2467–2475, 2015.
- Markus Heinonen, Cagatay Yildiz, Henrik Mannerström, Jukka Intosalmi, and Harri Lähdesmäki. Learning unknown ODE models with Gaussian processes. In Jennifer Dy and Andreas Krause, editors, *Proceedings of the 35th International Conference on Machine Learning*, volume 80 of *Proceedings of Machine Learning Research*, pages 1959–1968, Stockholm, Sweden, 2018. PMLR. URL <http://proceedings.mlr.press/v80/heinonen18a.html>.

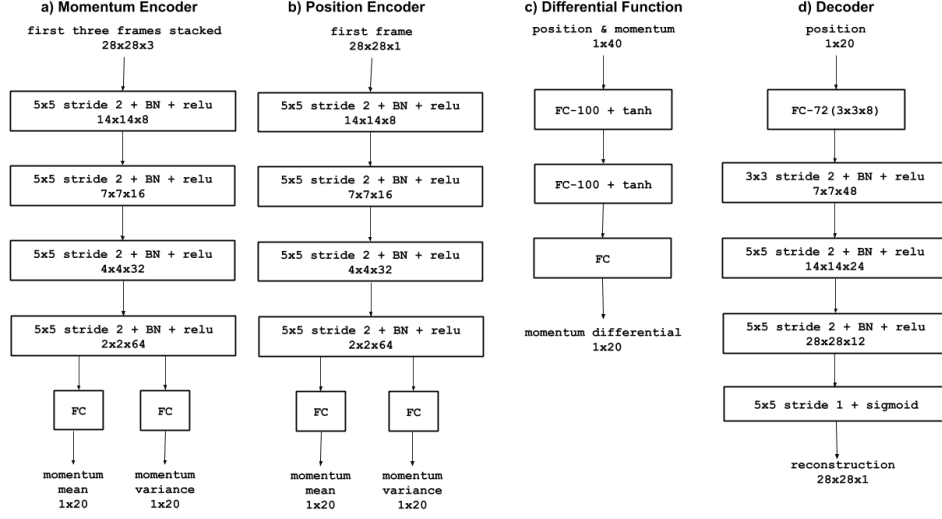


Figure 5: Rotating MNIST experiment neural architectures

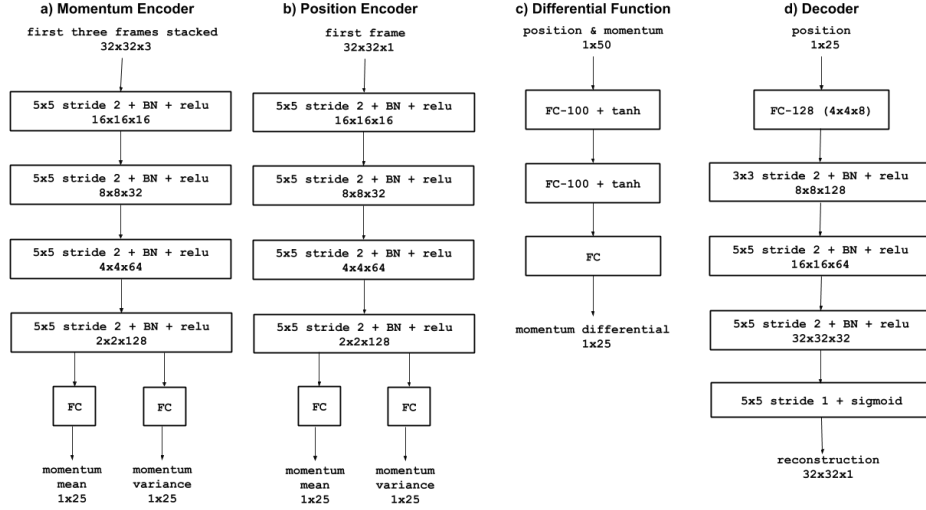


Figure 6: Bouncing balls experiment neural architectures

Jack M Wang, David J Fleet, and Aaron Hertzmann. Gaussian process dynamical models for human motion. *IEEE transactions on pattern analysis and machine intelligence*, 30(2):283–298, 2008.